Selective Targeting of Virus Replication by Proton Pump Inhibitors

Susan M. Watanabe[a], Lorna S. Ehrlich[a], Madeleine Strickland[b], Xiaofan Li[c], Veronica Soloveva[d], Arthur J. Goff[d], Charles B. Stauft[a], Sumita Bhaduri-McIntosh[c], Nico Tjandra[b] and Carol Carter[a#]

[a] Department of Microbiology and Immunology, Stony Brook University, Stony Brook, NY 11794-5222, USA; [b]Laboratory of Molecular Biophysics, National Heart, Lung, and Blood Institute, National Institutes of Health, Bethesda, MD, 20892, USA; [c] Department of Pediatrics, Division of Infectious Diseases and Department of Molecular Genetics and Microbiology, University of Florida, Gainesville, FL 32610, USA; [d]U.S. Army Medical Research Institute of Infectious Diseases, Frederick, MD, 21702-5011, USA.

[#]Corresponding authors:

Carol Carter: Department of Microbiology and Immunology, School of Medicine, Stony Brook University, Stony Brook, NY 11794-5222, USA; Tel. (631) 632-8801; email: carol.carter@stonybrook.edu

Nico Tjandra: Laboratory of Molecular Biophysics, National Heart, Lung, and Blood Institute, National Institutes of Health, Bethesda, MD, 20892, USA; Tel. (301) 402-3029; email: tjandran@nhlbi.nih.gov

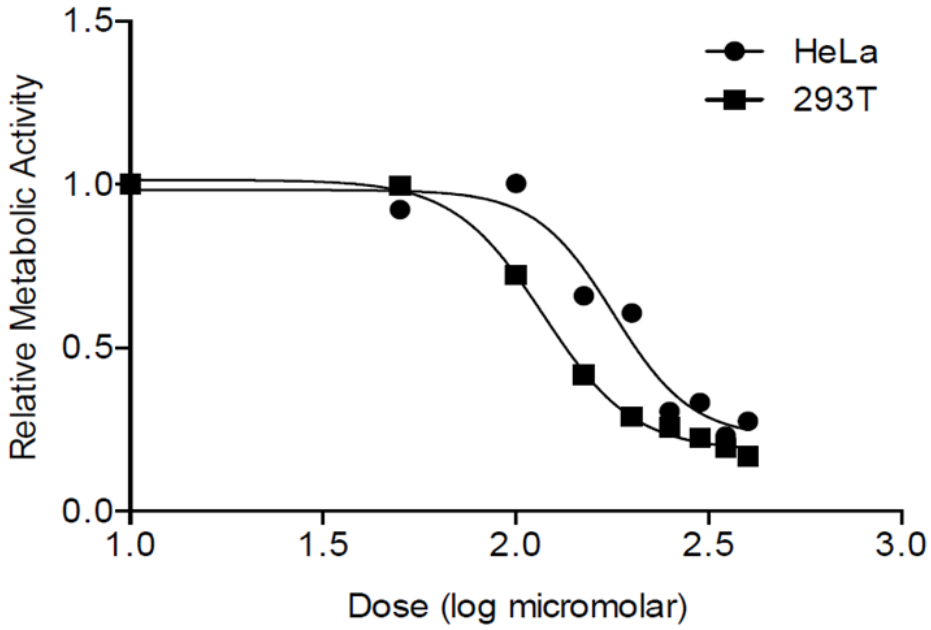

Supplementary Figure S1. Tenatoprazole effect on HeLa and HEK-293T cellular metabolism. Toxicity was determined by measuring metabolic activity (Roche, Cell Proliferation Reagent WST-1) after cells were grown for 24 hr with the drug. The CC_{50} values determined for Hela and 293T cells were 129 μM and 123 μM, respectively (Prism 6, Graph Pad Software Inc) with a goodness of fit R square values of 0.97 and 0.99, respectively.

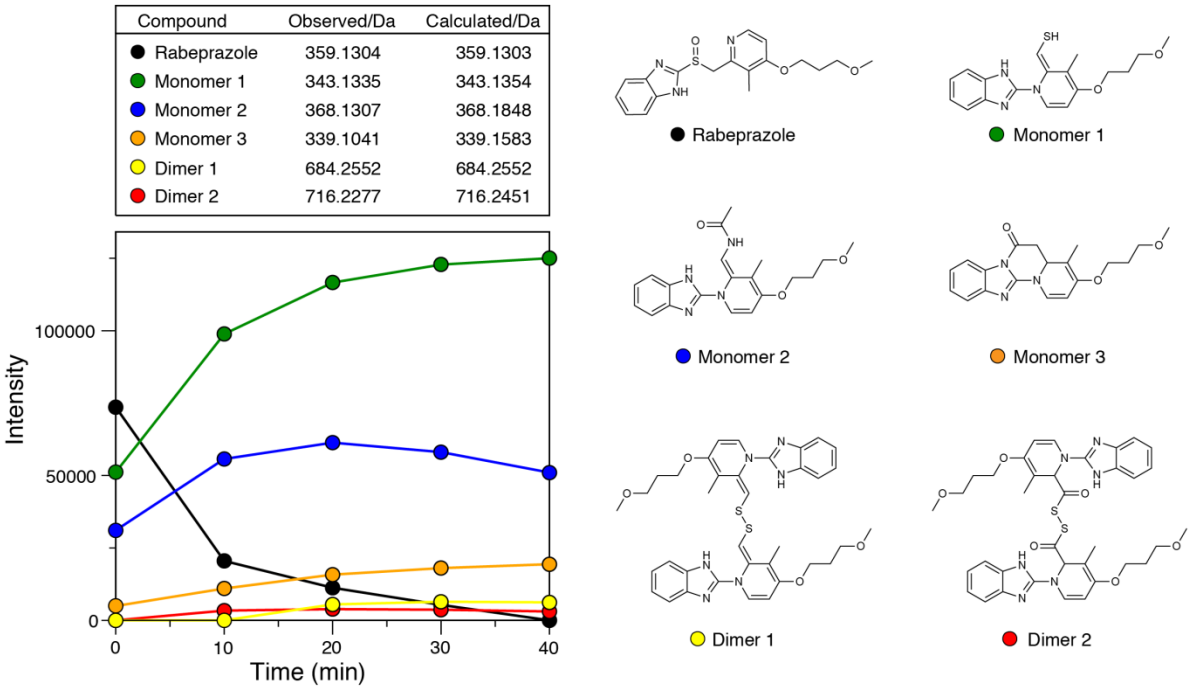

Supplementary Figure S2. Prodrug conversion to activated prazole. The formation of activated prazole was monitored using Ellman's reagent, which turns orange when it comes into contact with thiol (S-H) groups. Mass spec was used to detect the product in a time-dependent manner. Loss of prodrug correlates with the appearance of an active form. The molecules shown are suggestions likely to have the same molecular formula as the actual compounds.

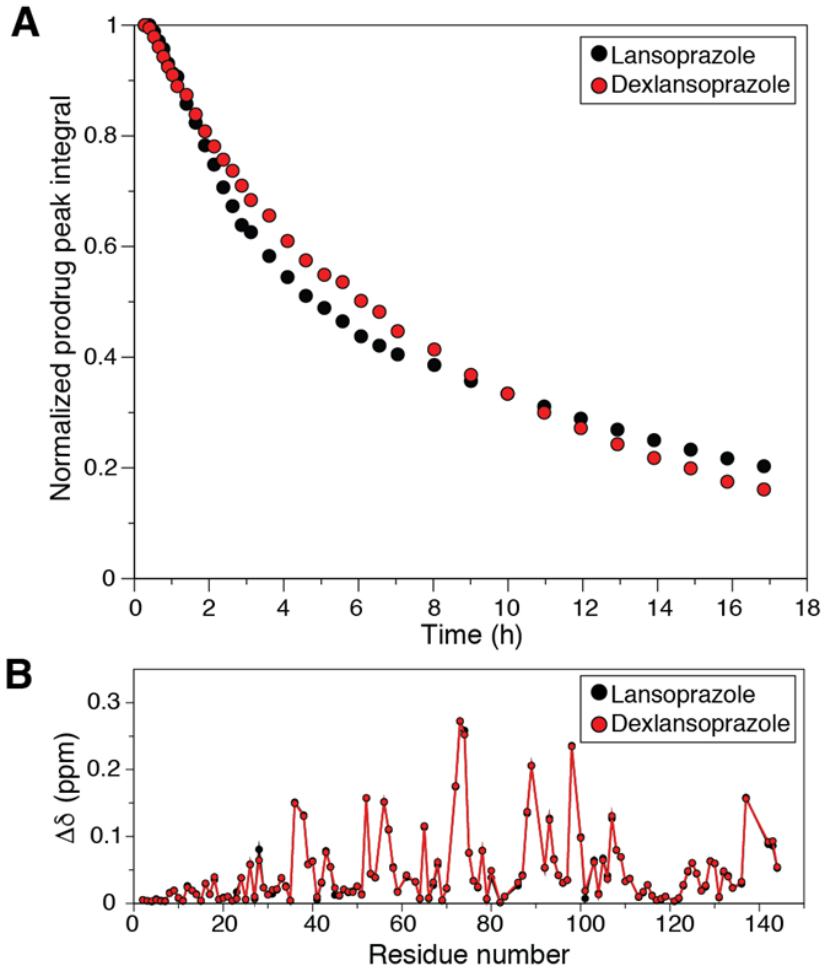

Supplementary Figure S3. Prazole degradation rate and chemical shift perturbations in Tsg101 UEV for racemic lansoprazole and single enantiomer dexlansoprazole. *Panel A*, Prodrug remaining at time intervals over a 17 hr examination period, measured using 1D NMR spectra. Peak heights were normalized to the initial reading for each prodrug and plotted against time. *Panel B*, Chemical shift perturbations in Tsg101 UEV complexed with lansoprazole and dexlansoprazole.

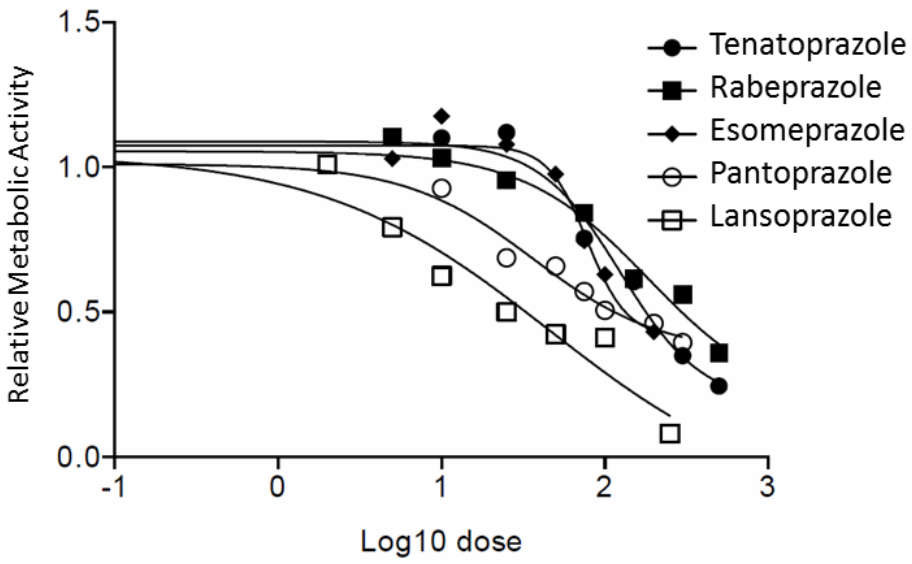

Supplementary Figure S4: Cellular metabolism measurements for tenatoprazole, esomeprazole, pantoprazole, rabeprazole, and lansoprazole. Metabolic activity was measured with a colorimetric assay (Roche, Cell Proliferation Reagent WST-1) after cells were grown for 24 hr with a drug. The CC_{50} values were: 125 μM (tenatoprazole), 150 μM (rabeprazole), 75 μM (esomeprazole), 40 μM (pantoprazole), 50 μM lansoprazole) as calculated by Prism 6, Graph Pad Software, Inc. The goodness of fit R square values varied from 0.94 to 0.97.

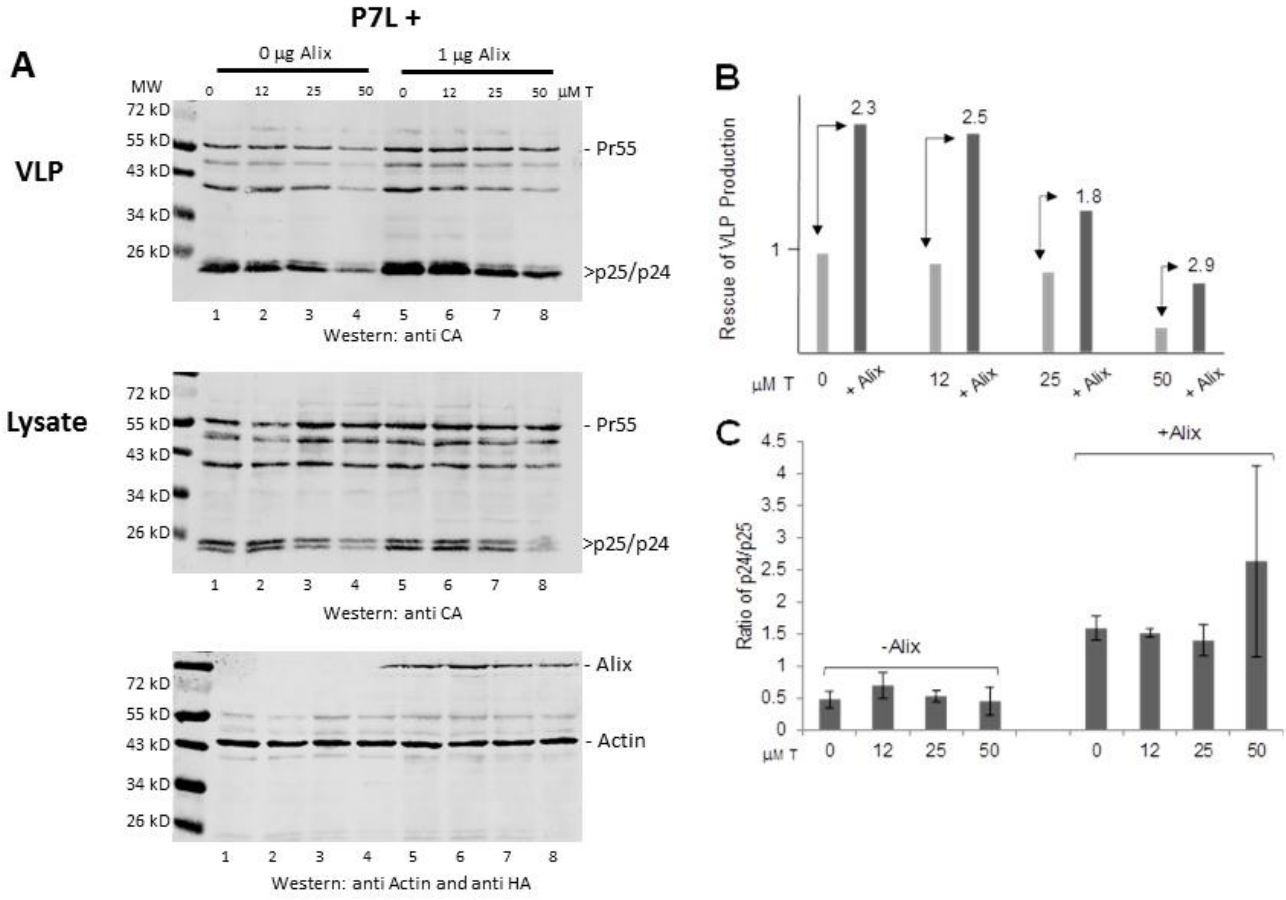

SUPPLEMENTARY FIGURE S5. Tenatoprazole effect on Alix-mediated rescue of pNL4-3-P7L-Gag release. ***Panel A***, 293T cells were treated with DMSO (lane 1) or tenatoprazole (Lanes 2 to 4) six hours prior to transfection with DNA encoding pNL4-3-P7L-Gag (lanes 1-8) and DNA encoding HA-tagged Alix (lanes 5-8). Western blot analysis of viral particles (*top*) and cell lysates (*bottom*) for CA p24-related proteins, actin and Alix. ***Panel B,*** Quantitative analysis of Alix rescue of VLP production. VLP release efficiency was determined in the absence and presence of Alix and normalized to cellular Gag accumulation plus VLP-associated Gag (*i.e.*, VLP/(VLP + cellular Gag). ***Panel C,*** Quantitative analysis of capsid maturation efficiency based on CAp25/p24 signals in the cell lysate.